

The inhibition effect of *o*-nitrophenol and Zn²⁺ system on corrosion of aluminium

D. Lakshmi,^{1*} J. Sathiyabama² and S. Rajendran^{2,3}

¹Department of Chemistry, M.V. Muthiah Government Arts College for Women, Dindigul-624001, Tamil Nadu, India

²Department of Chemistry, G.T.N.Arts College, Dindigul-624004, Tamil Nadu, India

³Department of Chemistry, St. Antony's college of arts and sciences for women, Dindigul-624005, Tamil Nadu, India

*E-mail: susairajendran@gmail.com

Abstract

Corrosion inhibition of aluminum (6061) in aqueous solution at pH 11 by *o*-nitrophenol–Zn²⁺ systems has been reported. The study was carried out using classical weight loss method, potentiodynamic polarization study and Fourier Transform Infra-red Spectroscopy (FTIR) Technique. Experimental results indicated that the presence of *o*-nitrophenol–Zn²⁺ inhibit the corrosion of Al(6061). The inhibition efficiency (*IE*) has been determined by the classical weight loss method. The maximum inhibition efficiency offered by the *o*-nitrophenol 250 ppm and Zn²⁺ 50 ppm system is 94%. To determine the values of Linear polarization resistance (LPR) and corrosion current (I_{corr}), potentiodynamic polarization study has been used and it reveal that the inhibitor act as anodic inhibitor and it controls the anodic reaction. The protective film has been characterized by FTIR, SEM, EDAX and AFM. The protective film consists of Al³⁺–*o*-nitrophenol complex on the anodic metal surface. By using Density Functional Theory (DFT) various quantum chemical parameters such as E_{HOMO} (highest occupied molecular orbital energy), E_{LUMO} (lowest unoccupied molecular orbital energy), energy gap (ΔE), electron affinity (*A*), ionization potential (*I*), absolute electronegativity (χ), global hardness (η), softness (*S*), fraction of electrons transferred (ΔN) have been calculated and discussed. The theoretical results were found to be consistent with the experimental data generated. The inhibition efficiency of the inhibitor is evaluated by weight loss method.

Keywords: aluminum(6061), potentiodynamic polarization, FTIR, SEM, EDAX, AFM, Density Functional Theory (DFT).

Received: March 5, 2017. Published: June 15, 2017.

doi: [10.17675/2305-6894-2017-6-3-2](https://doi.org/10.17675/2305-6894-2017-6-3-2)

Introduction

Corrosion, which is an predictable problem faced by almost all industries can be considered as one of the worst technical calamities of our time. Besides from its direct costs in dollars, corrosion is a serious problem because it definitely contributes to the

depletion of our natural resources. Corrosion studies have also become important due to increasing awareness of the need to conserve the world's metal resources [1–3]. Now-a-days more attention has been paid to control the metallic corrosion, due to increasing use of metals in all fields of technology. The economic aspect combined with security and environmental concerns have provided continuous motivation for the research community to develop new methods to reduce the impact of corrosion. Material selection is one of the general approaches used to prevent corrosion. Apart from specific requirements related to the actual application and/or the corrosion environment, there are also general criteria to be considered in material selection.

Aluminium and its alloys are the second largest used materials next to iron and its alloys due to their lightweight, strength, durability, formability and corrosion resistance. Prevention of corrosion of aluminium has been a subject of numerous studies due to their high technological value and wide range of industrial and house hold applications [4, 5].

The present work is undertaken:

- (1) To evaluate the inhibition efficiency (IE) of *o*-nitrophenol–Zn²⁺ system in controlling corrosion of Aluminium immersed in aqueous solution at pH 11 in the absence and presence of Zn²⁺ by weight-loss method.
- (2) To study the mechanism of corrosion inhibition by polarization study and AC impedance spectra.
- (3) To analyse the protective film by FTIR spectra, scanning electron microscope (SEM), Energy Dispersive Analysis of X-rays and atomic force microscope.
- (4) To propose the mechanism of corrosion inhibition based on the above results.

Materials and Methods

Preparation of inhibitor

1 g of commercially available inhibitor is dissolved in distilled water and then made up to 100 ml in a standard measuring flask by using double distilled water.

Preparation of specimens

Commercial aluminium specimens of dimensions 1.0×4.0×0.2 cm containing 95% pure aluminium were polished to mirror finish, degreased with trichloroethylene, and used for the weight loss method and for surface examination studies.

Weight loss method

Three aluminium specimens were immersed in the inhibitor solution at pH 11 in the presence and absence of Zn²⁺ ions. The weight of the specimen before and after immersion was determined using Shimadzu balance AY62. Inhibition efficiency (IE) (+ or – 5%) (room temperature 25°C) was calculated from the relationship $IE = (1 - W_2/W_1) \times 100$,

where W_1 = corrosion rate in the absence of inhibitor, and W_2 = corrosion rate in the presence of the inhibitor.

Potentiodynamic polarization study

Polarization study was carried out in Electrochemical Impedance analyzer model CHI 660A three electrode cell assembly was used. The working electrode was used as a rectangular specimen of mild steel with one face of the electrode of constant 1 cm^2 area exposed. A saturated calomel electrode (SCE) was used as the reference electrode and a rectangular platinum foil was used as the counter electrode. Polarization curves were recorded after doing iR compensation. The corrosion parameters such as corrosion potential (E_{corr}), corrosion current (I_{corr}) and Tafel slopes (anodic = b_a and cathodic = b_c) and Linear polarization resistance (LPR) were calculated. During the polarization study, the scan rate (V/s) was 0.005; hold time at E_f (s) was zero and quiet time (s) was 2.

FTIR spectra

These spectra were recorded with the Perkin-Elmer-1600 spectrophotometer. The FTIR spectrum of the protective film was recorded by carefully removing the film mixed it with KBr and making the pellet.

Scanning Electron Microscopic studies (SEM)

The mild steel specimen immersed in blank and in the inhibitor solution for a period of one day was removed, rinsed with double distilled water, dried and observed in a scanning electron microscope to examine the surface morphology. The surface morphology measurements of the mild steel were examined using Tescon, Vega3, and USA computer controlled scanning electron microscope. The elemental analysis of the mild steel surface at the same condition was carried out using an energy dispersive X-ray analyzer (EDAX) [Brucker, Nano, GMBH, Germany] unit attached to the SEM machine.

Atomic Force Microscopy (AFM)

Atomic Force Microscope (AFM) is a new technique which allows metal surface to be imaged at higher resolutions and accuracies than ever before. The carbon steel specimen immersed in blank and in the inhibitor system for one day. The carbon steel specimens were removed, rinsed with double distilled water, dried, and subjected to the surface examination. Veeco Innova model was used to observe the carbon steel surface in tapping mode, using cantilever with linear tips. The scanning area in the images was $50 \mu\text{m} \times 50 \mu\text{m}$ and the scan rate was 0.6 Hz s^{-1} . A two dimensional, and a three dimensional topography of metal surface films gave various roughness parameters of the film.

Results and Discussion

Weight Loss Method

Inhibition efficiencies ($IE\%$) of *o*-nitrophenol– Zn^{2+} systems in controlling corrosion of aluminium (6061) immersed in aqueous solution at pH 11 in the presence and absence of inhibitor system (immersion period – 1 day) are given in Tables 1 and 2. It is obvious that *o*-nitrophenol alone has poor inhibition efficiency. In the presence of 50 ppm concentration of Zn^{2+} the IE of *o*-nitrophenol becomes effective. A synergistic effect exists between *o*-nitrophenol and Zn^{2+} . For example 50 ppm of *o*-nitrophenol has only 12% IE whereas 50 ppm of Zn^{2+} has 15% IE . However their combination has 81% IE . This denotes that a synergistic effect exists between *o*-nitrophenol and Zn^{2+} [6–9].

Table 1. Corrosion rates (CR) and the inhibition efficiency (IE) obtained by weight loss method of aluminium(6061) immersed in aqueous solution at pH 11. Temperature: 25°C. Inhibitor system: *o*-nitrophenol– Zn^{2+} (0 ppm). Immersion period: 1 day; pH 11.

<i>o</i> -Nitrophenol (ppm)	Zn^{2+} (ppm)	CR (mdd)	IE (%)
0	0	13.63	–
50	0	11.99	12
100	0	10.90	20
150	0	9.13	33
200	0	7.63	44
250	0	6.41	53

Table 2. Corrosion rates (CR) and the inhibition efficiency (IE) obtained by weight loss method of aluminium(6061) immersed in aqueous solution at pH 11. Temperature: 25°C. Inhibitor system: *o*-nitrophenol– Zn^{2+} (50 ppm). Immersion period: 1 day; pH 11.

<i>o</i> -Nitrophenol (ppm)	Zn^{2+} (ppm)	CR (mdd)	IE (%)
0	0	13.63	–
0	50	11.58	15
50	50	2.58	81
100	50	2.04	85
150	50	1.77	87
200	50	1.36	90
250	50	0.82	94

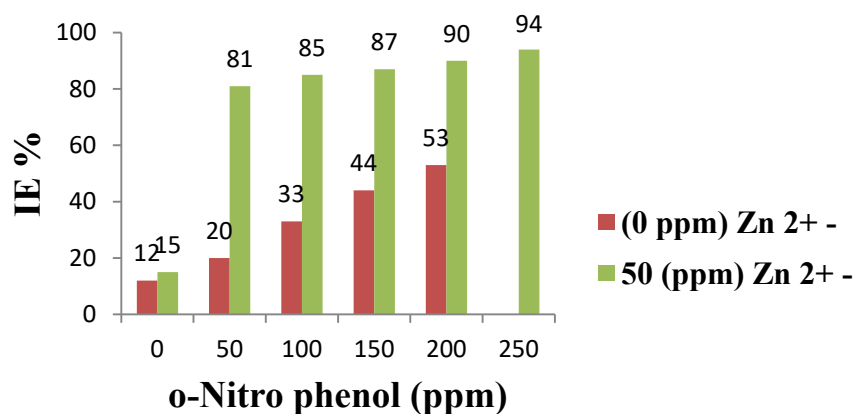


Figure 1. Inhibition efficiencies (*IE* %) of aluminium(6061) immersed in various solutions.

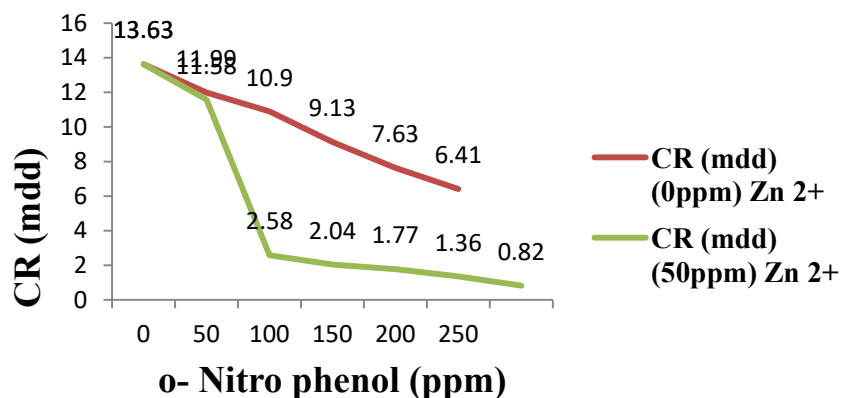


Figure 2. Corrosion rates (*CR*) of aluminium(6061) immersed in various solutions.

Potentiodynamic Polarization Study

Electrochemical studies such as Polarization study has been used to confirm the formation of protective film formed on the metal surface during corrosion inhibition process. If a protective film forms on the metal surface, the linear polarization resistance value (*LPR*) will increase and corrosion current value (I_{corr}) decrease [10–14].

Monitoring of *LPR* [15] is a rapid method of measuring corrosion rate. Since the rate of corrosion can be identified in minutes using this method, an immediate measuring system can be implemented. A fluid's electrical conductivity is associated with its ability to cause corrosion. In this test, two to three electrode probes are included in the process system where the electrodes are isolated electronically. Typically, 20 mV is put into the elements to produce current. With this, the linear polarization resistance refers to the applied potential ratio with the current level resulting from the process. The output or resistance is inversely proportional to the rate of corrosion.

The following equation shows conductor electrical resistance:

$$R = V/I$$

Where, R is the instantaneous resistance; V is the applied voltage; I is the instantaneous current that exists in between the electrodes.

If the electrodes are corroding at elevated rates while metal ions easily pass within the solution, this results in low levels of linear polarization resistance and high current, which is equivalent to high levels of corrosion. This also allows for instant feedback, which leads to more effective monitoring and evaluation of corrosion in various operations. Electrochemical corrosion potential (ECP) is the voltage difference between a metal immersed in a given environment and an appropriate standard reference electrode (SRE), or an electrode which has a stable and well-known electrode potential. ECP is used to list metals or alloys based on their corrosion resistance. Electrochemical corrosion potential is also known as rest potential, open circuit potential or freely corroding potential, and in equations it is represented by E_{corr} .

The potentiodynamic polarization curves of aluminium(6061) immersed in aqueous solution at pH 11 (NaOH) in the absence and presence of inhibitors are shown in Figure 3. The corrosion parameters are shown in Table 3. When aluminium(6061) was immersed in aqueous solution at pH 11 (NaOH) the corrosion potential was -1573 mV vs. SCE. When *o*-nitrophenol (250 ppm) and Zn^{2+} (50 ppm) were added to the above system the corrosion potential shifted to the noble side -1427 mV vs. SCE. This indicates that a film is formed on the anodic sites of the metal surface. This film controls the anodic reaction of metal dissolution by forming Al^{3+} *o*-nitrophenol complex on the anodic sites of the metal surface [16]. Further the LPR values increases from 215 Ohm cm^2 to 1735.4 Ohm cm^2 . The corrosion current decreases from $2848 \times 10^{-4} \text{ A/cm}^2$ to $254.9 \times 10^{-4} \text{ A/cm}^2$. Thus the Polarization study confirms the formation of protective film on the metal surface.

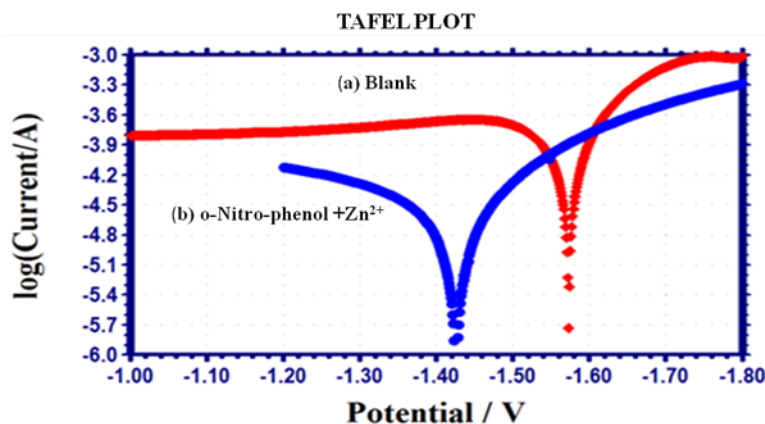


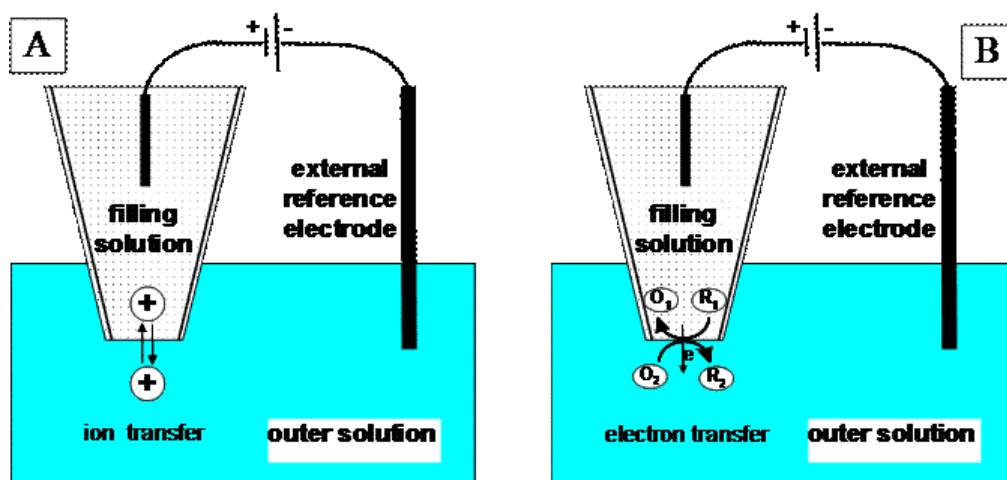
Figure 3. Polarization curves of aluminum immersed in various solutions. (a) blank; (b) aqueous solution at pH 11 containing *o*-nitrophenol (250 ppm) + Zn^{2+} (50 ppm).

Table 3. Corrosion parameter of aluminium(6061) immersed in aqueous solution at pH 11 in the presence and absence of inhibitor system obtained by Potentio-dynamic Polarization Study.

System	E_{corr} mV vs SCE	b_c mV/decade	b_a mV/decade	LPR Ohm cm^2	I_{corr} A/ cm^2
Blank pH 11	-1573	0.18047	0.6406	215.0	2848×10^{-4}
<i>o</i> -nitrophenol (250 ppm) + Zn^{2+} (50 ppm)	-1427	0.1636	0.2822	1735.4	254.9×10^{-4}

AC impedance spectra

AC impedance spectra (electrochemical impedance spectra) have been used to confirm the formation of protective film on the metal surface. If a protective film is formed on the metal surface, charge transfer resistance (R_t) increases. Charge transfer resistance has to do with the process of electron transfer from one phase (*e.g.* electrode) to another (*e.g.* liquid).

**Figure 4.** Electron transfer from electrode to liquid.

[A nanopipette is filled with an aqueous solution and immersed in an outer solution immiscible with water. By applying voltage between the reference electrode inside the pipette and the external reference, one can induce either ion transfer (A) or electron transfer (B) across the liquid/liquid interface]. Double layer capacitance value (C_{dl}) decreases and impedance $\log(Z/\text{Ohm})$ value increases. Double-layer capacitance is the storing of electrical energy by means of the electrical double layer effect. This electrical phenomenon appears at the interface between a conductive electrode and an adjacent liquid electrolyte as observed, for example, in a super capacitor.

It is observed from Figure 5 that when aluminium(6061) immersed in aqueous solution at pH 11 (NaOH) two semi circles were observed. This is characteristic of a protective film formed and then broken. The breaking of the film is due to the presence of

corrosive ions present in solution. The equivalent circuit diagram for such system is shown in Scheme 1.

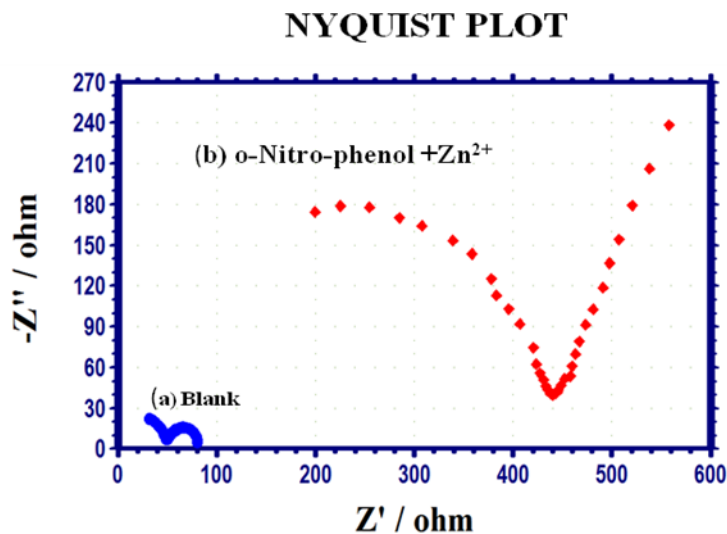
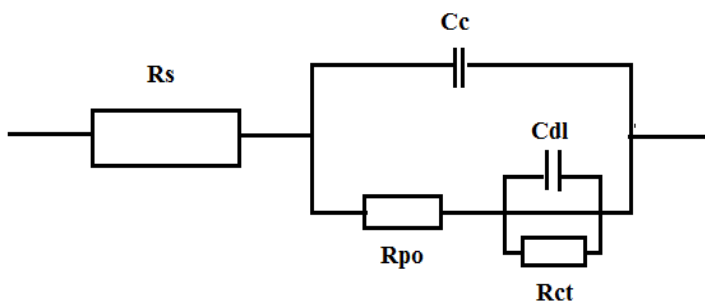


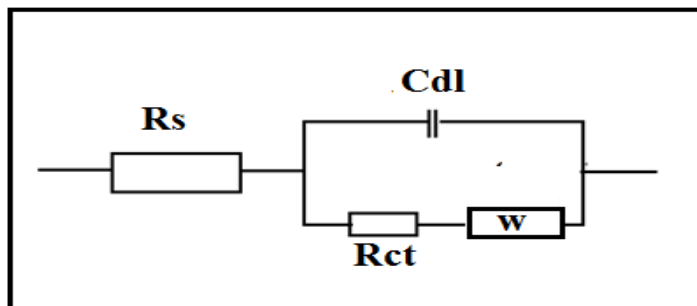
Figure 5. AC impedance spectra of aluminium(6061) immersed in solution (Nyquist plot). (a) blank; (b) aqueous solution at pH 11 containing *o*-nitrophenol (250 ppm) + Zn^{2+} (50 ppm).



Scheme 1. Equivalent circuit for a failed coating. C_c – the capacitance of the intact coating, R_{po} – pore resistance, R_{ct} – charge transfer resistance, R_s – solution resistance, C_{dl} – double layer capacitance.

The AC impedance spectra of aluminium(6061) immersed in aqueous solution at pH 11 (NaOH) in the presence and absence of inhibitors (*o*-nitrophenol– Zn^{2+}) are shown in Figure 5 (Nyquist plot) and Figure 6 (a,b) [Bode plots]. The AC impedance parameters namely charge transfer resistance (R_t) and double layer capacitance value (C_{dl}) derived from Nyquist plots and the impedance $\log(Z/\text{Ohm})$ values derived from Bode plots respectively are given in Table 4. The fact that when the inhibitors [*o*-nitrophenol (250 ppm) + Zn^{2+} (50 ppm)] are added, the charge transfer resistance increases from 50.81 Ohm cm^2 to 373.2 Ohm cm^2 . The C_{dl} value decreases from $9.8405 \times 10^{-8} \text{ F/cm}^2$ to $1.339 \times 10^{-8} \text{ F/cm}^2$. The impedance value [$\log(Z/\text{Ohm})$] increases from 1.908 to 2.790. This observations lead to the conclusion that a protective film is formed on the metal surface [17, 18] in the presence of inhibitors [*o*-nitrophenol– Zn^{2+}] form a stable protective film formed on the metal surface. Equivalent circuit diagram for such a system is shown in

Scheme 2. The circuit models a cell where polarization is due to a combination of kinetic and diffusion process.



Scheme 2. R_s – solution resistance, R_{ct} – charge transfer resistance, W – Warburg diffusion resistance, C_{dl} – Double layer capacitance.

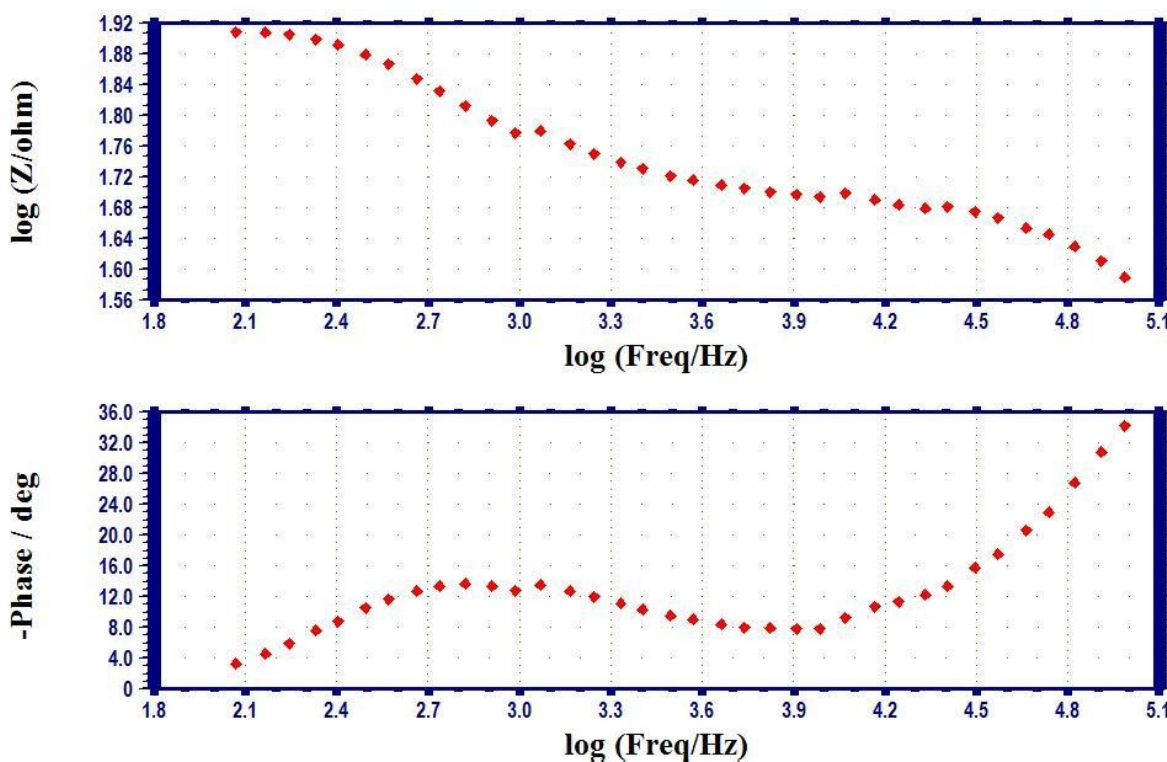


Figure 6(a). AC impedance spectrum of aluminium(6061) immersed in blank solution at pH 11 (Bode plot).

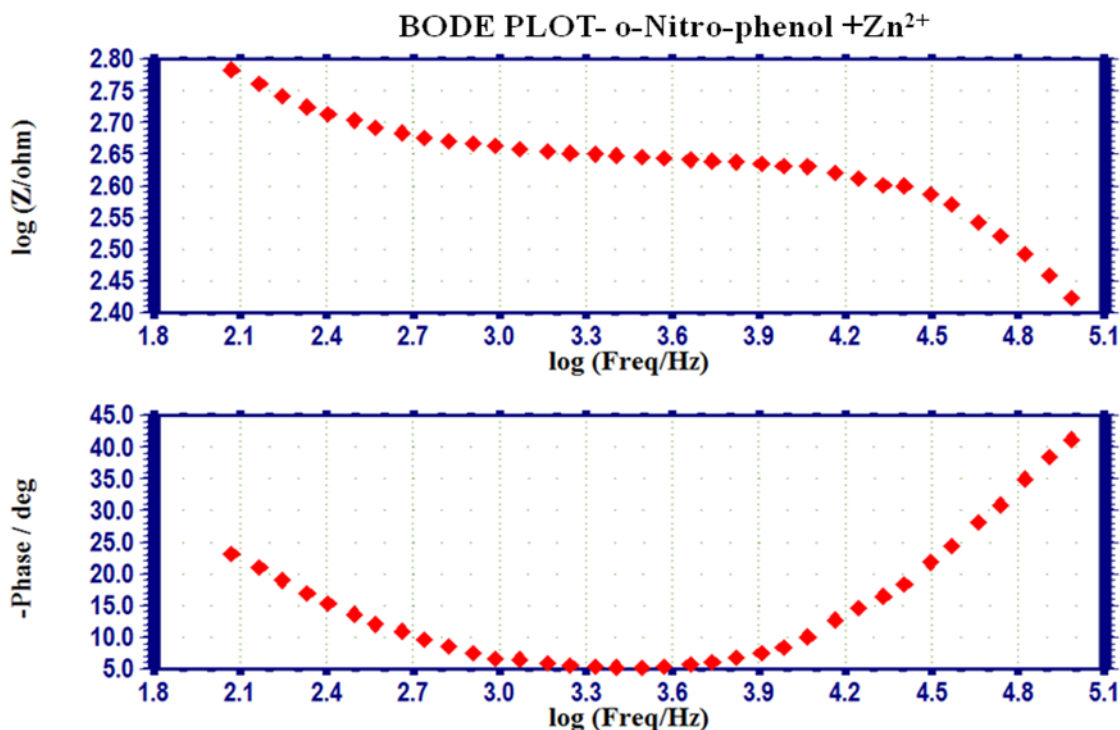


Figure 6(b). AC impedance spectrum of Aluminium(6061) immersed in *o*-nitrophenol–Zn²⁺ system (Bode plot).

Table 4. Corrosion parameters of aluminium (6061) immersed in aqueous solution at pH 11 in the absence and presence of inhibitor system obtained from AC impedance spectra.

System	Nyquist Plot		Bode Plot
	R_t Ohm cm ²	C_{dl} F/cm ²	Impedance value log(Z/Ohm)
Blank	50.81	9.8405×10^{-8}	1.908
<i>o</i> -Nitrophenol (250 ppm) + Zn ²⁺ (50 ppm)	373.2	1.339×10^{-8}	2.790

FTIR Spectra

FTIR spectra have been used to analyze the protective film formed on the metal surface [19–21]. The FTIR spectrum of *o*-nitrophenol is shown in Figure 7. The broad band at 3430 cm⁻¹ observed in the spectrum of *o*-nitrophenol (KBr) indicates the –OH stretching vibration. A peak at 1613 cm⁻¹ is attributed for the –N=O stretching vibration.

The FTIR spectrum of the film formed on the surface of aluminium(6061) immersed in *o*-nitrophenol (250 ppm) and Zn²⁺ (50 ppm) at pH 11 is shown in Figure 8. The –OH stretching frequency appears at 3429 cm⁻¹. The –N=O stretching frequency has shifted from 1613 cm⁻¹ to 1594 cm⁻¹ which indicates that *o*-nitrophenol has coordinated with Al³⁺ through the oxygen atom of the –N=O group in *o*-nitrophenol. So *o*-nitrophenol has

coordinated with Al^{3+} through the nitro oxygen resulting in the formation of Al^{3+} -*o*-nitrophenol complex. The band at 615 cm^{-1} may be due to the metal–oxygen stretching vibration and the band at 1405 cm^{-1} may be due to in plane vibrations of $-\text{OH}$ group in $\text{Zn}(\text{OH})_2$. This indicates the presence of $\text{Zn}(\text{OH})_2$ on the metal surface. There is also possibility of formation of $\text{Al}(\text{OH})_3$ precipitate on the metal surface.

When aluminium(6061) is immersed in this solution the Zn^{2+} -*o*-nitrophenol complex diffuses from the bulk of the solution towards the metal surface. Zn^{2+} -*o*-nitrophenol complex is converted into Al^{3+} -*o*-nitrophenol complex on the metal surface. Zn^{2+} is released and $\text{Zn}(\text{OH})_2$ is formed. Thus a protective film consisting of Al^{3+} -*o*-nitrophenol complex is formed on the anodic metal surface. [Between pH 8 and 12 the ions polymerise by means of OH bridges and each aluminium is octahedrally coordinated. Thus $\text{Al}(\text{OH})_3$ dissolves in NaOH but is reprecipitated by the addition of carbon dioxide.] [21a]

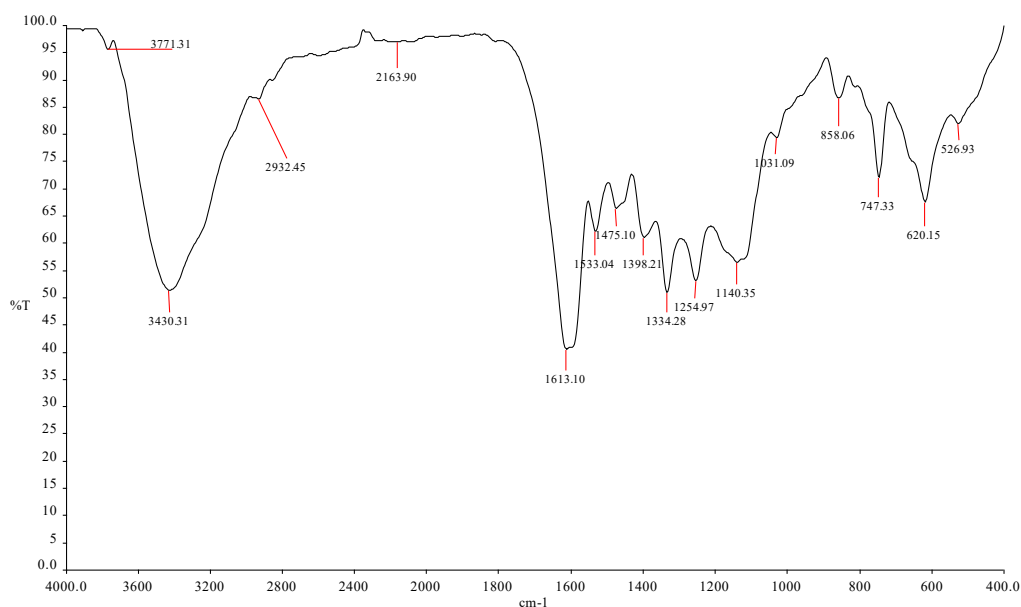


Figure 7. FTIR spectrum of pure *o*-nitrophenol.

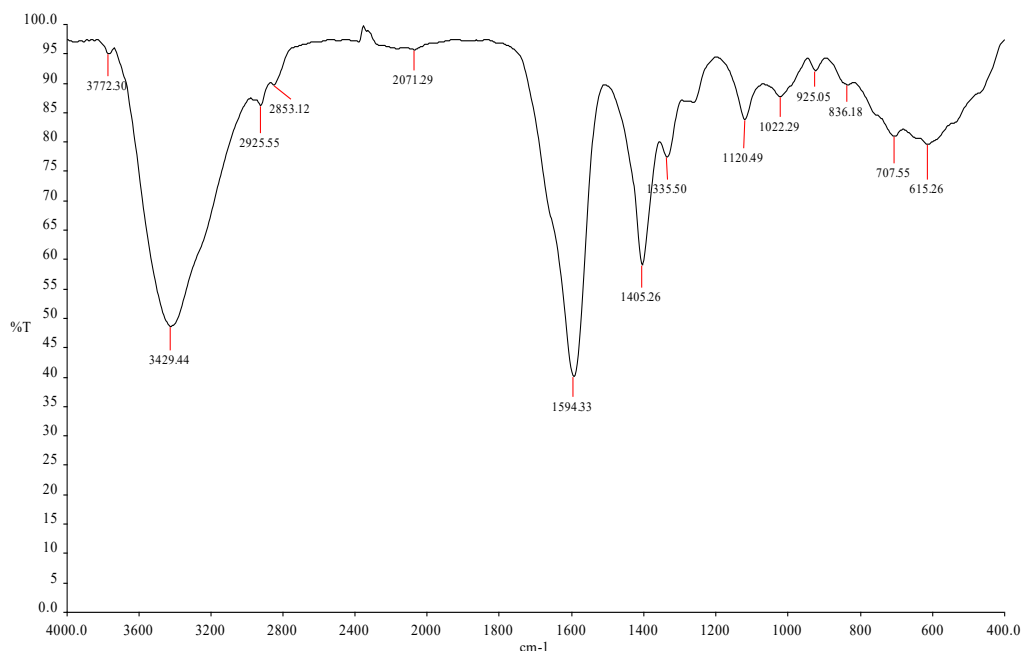


Figure 8. FTIR Spectrum of the film formed on the surface of aluminium(6061) immersed in *o*-nitrophenol (250 ppm) and Zn^{2+} (50 ppm) at pH 11.

Atomic Force Microscopy characterization

Atomic force microscopy (AFM) is an effective method for investigation and collection of roughness statistics from a variety of surfaces. AFM image analysis was performed to obtain the average roughness, R_a (the average deviation of all points roughness profile from a mean line over the evaluation length), root-mean-square roughness, R_q (the average of the measured height deviations taken within the evaluation length and measured from the mean line) and the maximum peak-to-valley (P-V) height values (largest single peak-to-valley height in five adjoining sampling heights). R_q is much more sensitive than R_a to large and small height deviations from the mean [22].

The two dimensional (2D), three dimensional (3D) AFM morphologies and the AFM cross-sectional profile for polished aluminium(6061) surface, aluminium(6061) surface immersed in aqueous solution at pH 11 (blank) and aluminium(6061) surface immersed in aqueous solution at pH 11 containing *o*-nitrophenol– Zn^{2+} (50 ppm) are shown in Figure 9, 10 and 11, respectively.

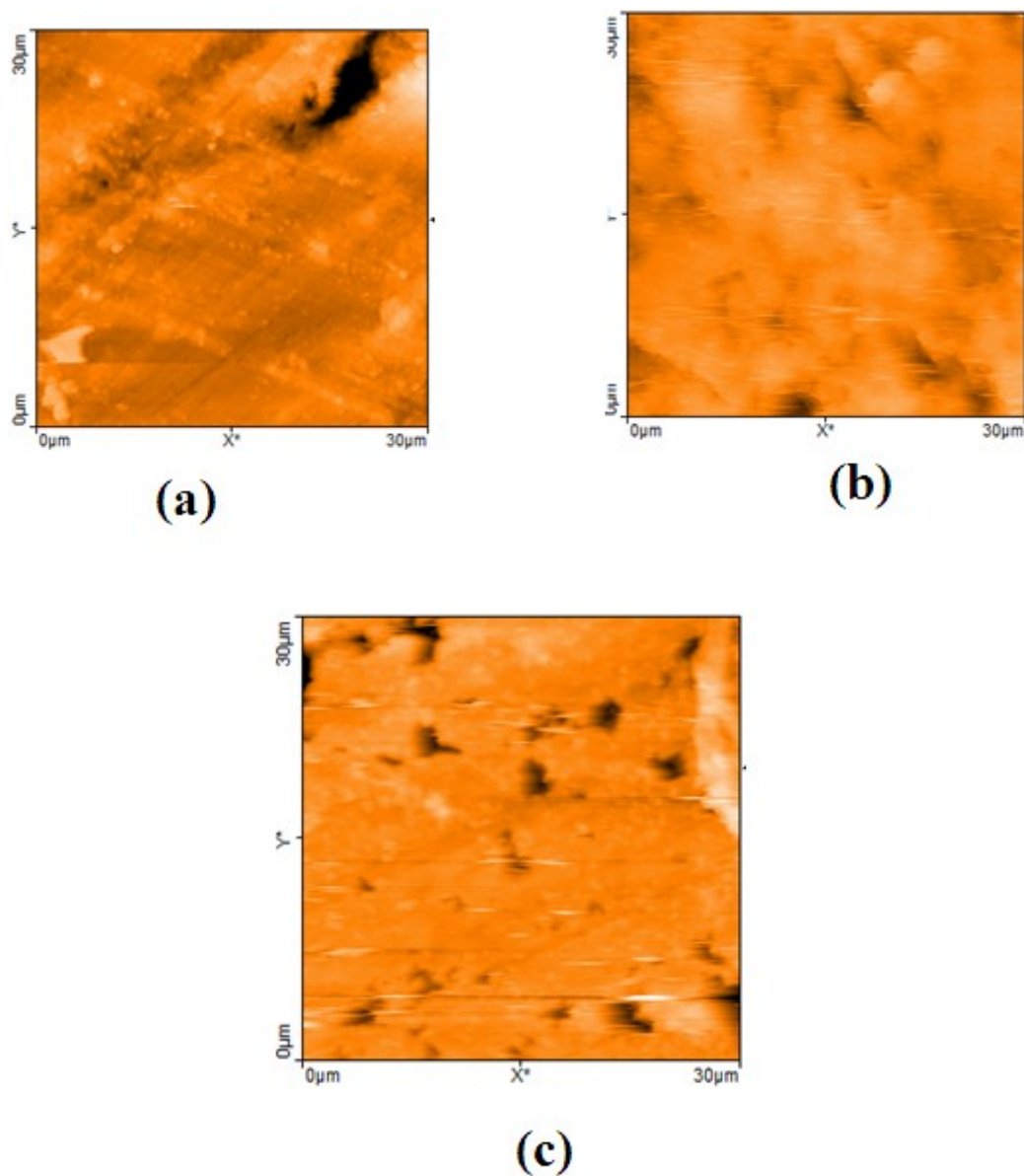


Figure 9. Two dimensional AFM images of the surface of (a) Polished aluminium (6061); (b) Aluminium(6061) immersed in aqueous solution at pH 11 (blank); (c) Aluminium (6061) immersed in solution containing *o*-nitrophenol (250 ppm)+Zn²⁺(50 ppm) at pH 11.

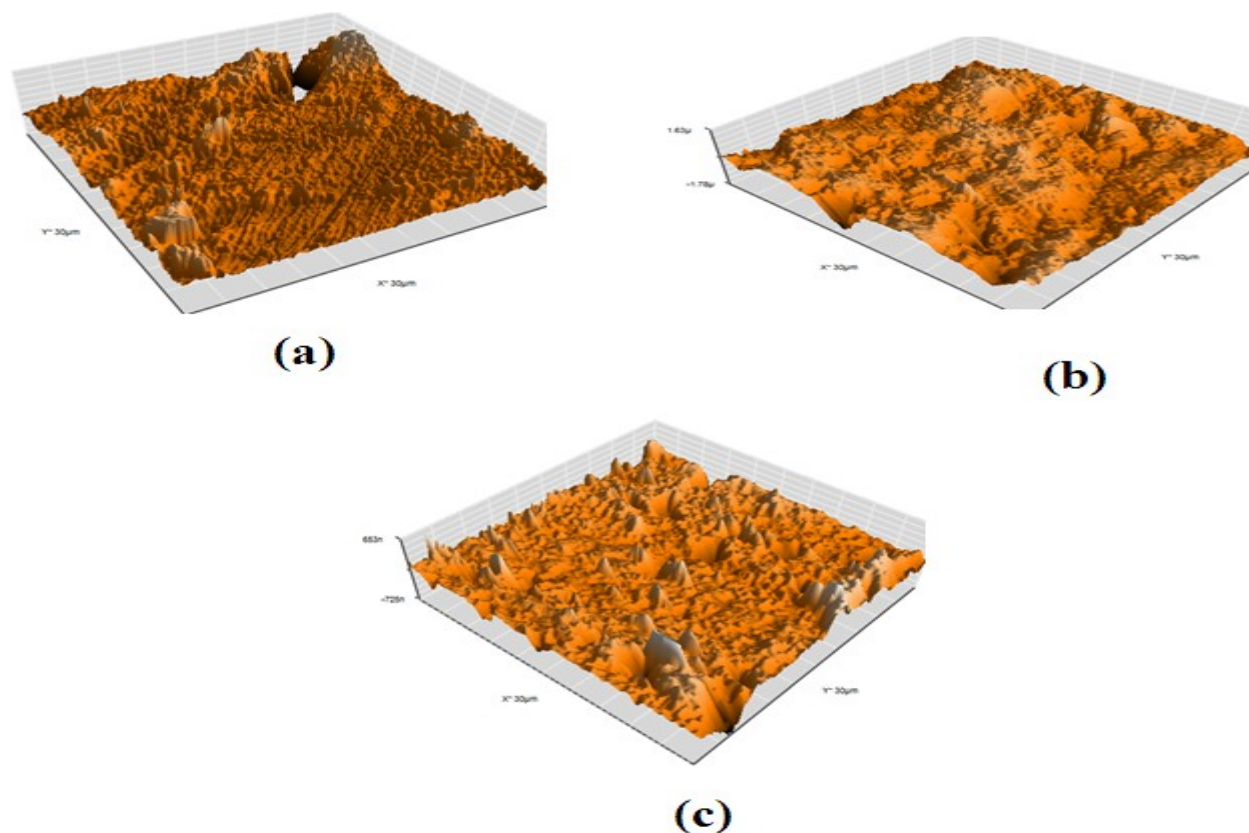


Figure 10. Three dimensional AFM images of the surface of (a) Polished aluminium(6061); (b) Aluminium(6061) immersed in aqueous solution at pH 11(blank); (c) Aluminium(6061) immersed in solution containing *o*-nitrophenol (250 ppm)+Zn²⁺(50 ppm) at pH 11.

The R_q , R_a and P-V values for aluminium(6061) surface immersed in different environment are summarized in Table 5.

Table 5. AFM data for aluminium(6061) surface immersed in uninhibited environment.

Sample	RMS (R_q) Roughness (nm)	Average (R_a) Roughness (nm)	Maximum Peak-to- Valley height (nm)
Polished aluminium(6061) (control)	41.46	32.56	132.41
Aluminium(6061) immersed in aqueous solution at pH 11 (blank)	267.62	239.13	948.62
Aluminium(6061) immersed in aqueous solution at pH 11 + <i>o</i> -nitrophenol + Zn ²⁺ (50ppm)	56.824	37.972	192.33

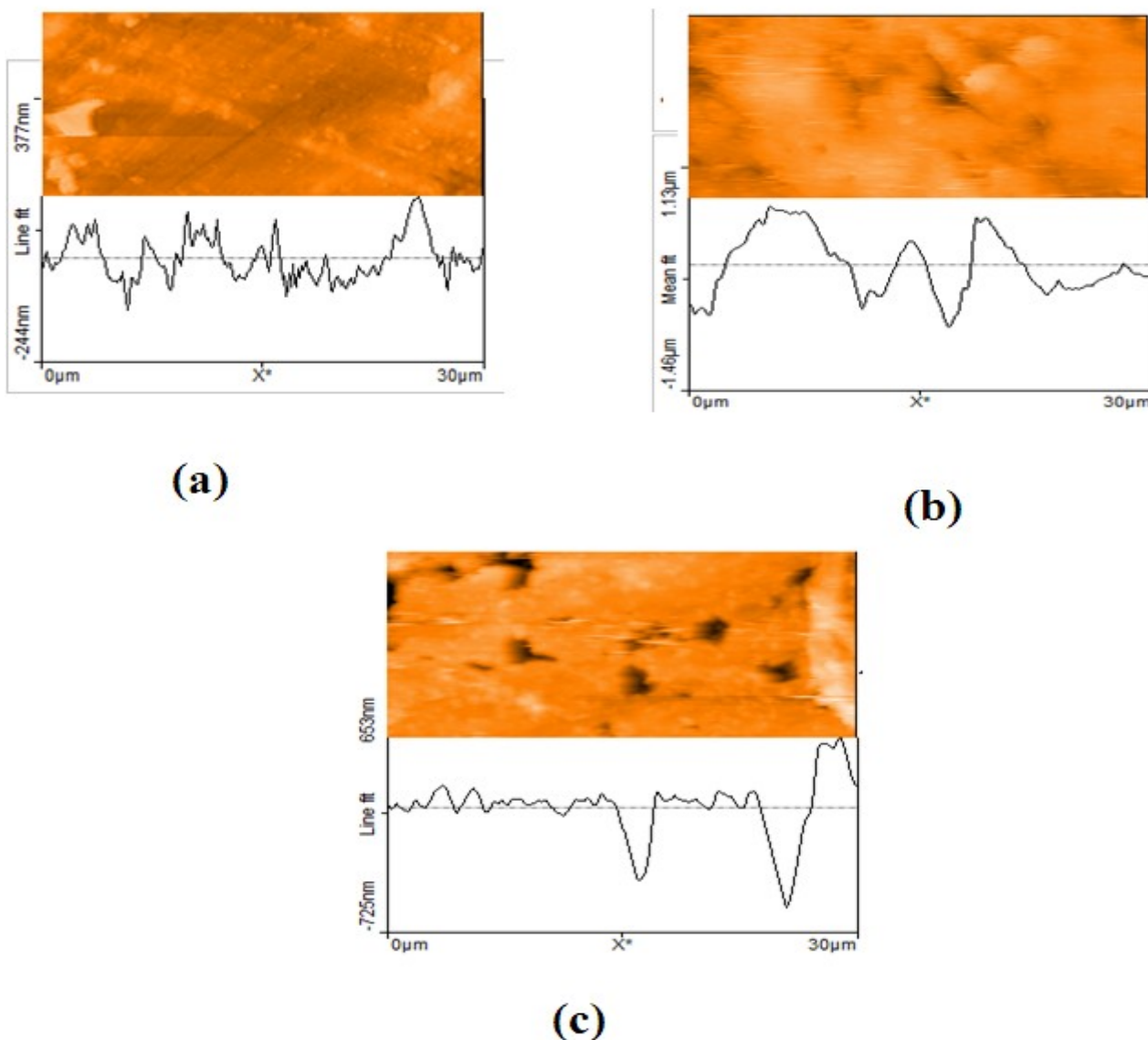


Figure 11. AFM cross sectional images of the surface of (a) Polished aluminium(6061); (b) Aluminium(6061) immersed in aqueous solution at pH 11 (blank); (c) Aluminium(6061) immersed in solution at pH 11 containing *o*-nitrophenol (250 ppm)+Zn²⁺ (50 ppm).

In Figures 9a, 10a and 11a the surface topography of uncorroded metal surface is shown. The values of R_q , R_a and P-V height for the polished aluminium(6061) surface are 41.46 nm, 32.56 nm and 132.41 nm, respectively. The data indicate a homogeneous surface. The slight roughness formed on the polished aluminium(6061) surface is due to atmospheric corrosion.

Figures 9b, 10b and 11b show the pitted, corroded metal surface in the absence of the inhibitor immersed in aqueous solution at pH 11. The R_q , R_a and P-V height values for the aluminium(6061) surface immersed in aqueous solution at pH 11 are 267.62 nm, 239.13 nm and 948.62 nm respectively. These data indicate that aluminium(6061) surface immersed in aqueous solution at pH 11 has severe surface roughness than the polished

metal surface, which shows that the unprotected aluminium(6061) surface is too rough due to the corrosion of the aluminium in aqueous solution at pH 11 environment.

Figures 9c, 10c and 11c show the complete changes on the aluminium(6061) surface after immersion in aqueous solution at pH 11 containing *o*-nitrophenol–Zn²⁺ (50 ppm). The R_q , R_a and P-V height values for the aluminium(6061) surface immersed in the above experimental solution are 56.824 nm, 37.972 nm and 192.33 nm respectively. The R_q , R_a and P-V height values are considerably less in the inhibited environment compared to the uninhibited environment. So, these parameters confirm that the surface is smoother than the uninhibited environment. The smoothness of the surface is due to the formation of a compact protective film of Al³⁺–*o*-nitrophenol complex and Zn(OH)₂ on the metal surface, thereby inhibiting the corrosion of aluminium(6061) [23, 24].

The R_q , R_a and P-V values of aluminium(6061) immersed in the aqueous solution at pH 11 in the presence of inhibitors, are greater than the R_q , R_a and P-V values of polished metal surface. This confirms the presence of the film on the metal surface, which is protective in nature.

Scanning Electron Microscope (SEM)

SEM provides a pictorial representation of the surface. SEM micrographs [25–27] are used to examine the nature of the surface film formed on the metal in the presence and absence of inhibitors. The SEM images of magnifications (50 μm) of aluminium(6061) and aluminium(6061) immersed in aqueous solution at pH 11 for 1 day in the presence and absence of inhibitor system are shown in Figure 12 as images (a,b and c) respectively. In Figure 12(a) the image arrived by the SEM micrographs of polished aluminium(6061) surface illustrates the smooth surface of the metal and the absence of any corrosion products which could form on the metal surface. The image shown in Figure 12(b) denotes the effect of SEM micrographs of aluminium(6061) immersed in aqueous solution at pH 11, verifies that the surface is corroded in an inhibitor free solution. The presence of *o*-nitrophenol–Zn²⁺ (50 ppm) mixture in aqueous solution at pH 11, suppresses the rate of corrosion which results in the formation of insoluble complex formed on the surface of the metal (Al³⁺–*o*-nitrophenol complex) is shown in Figure 12(c).

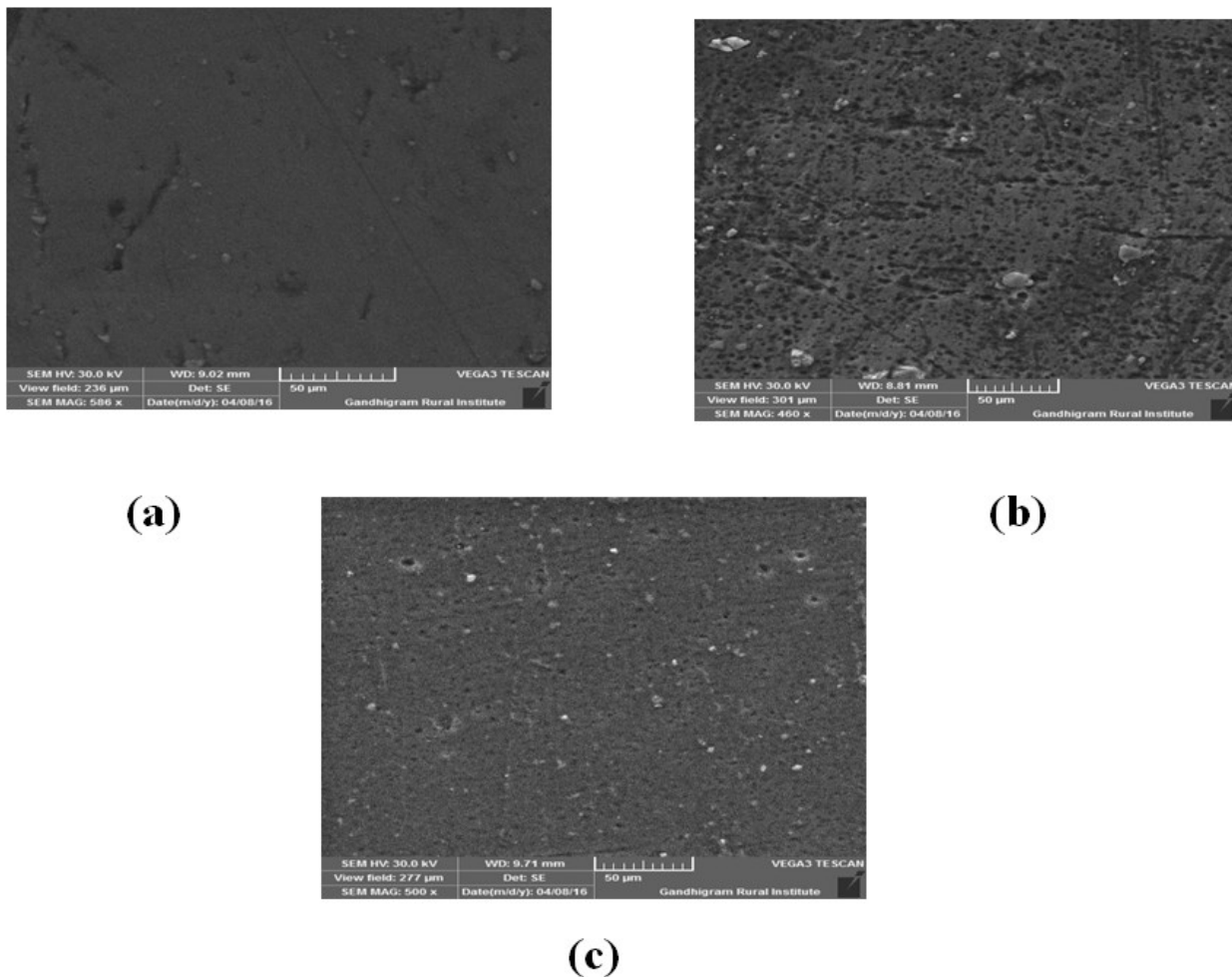


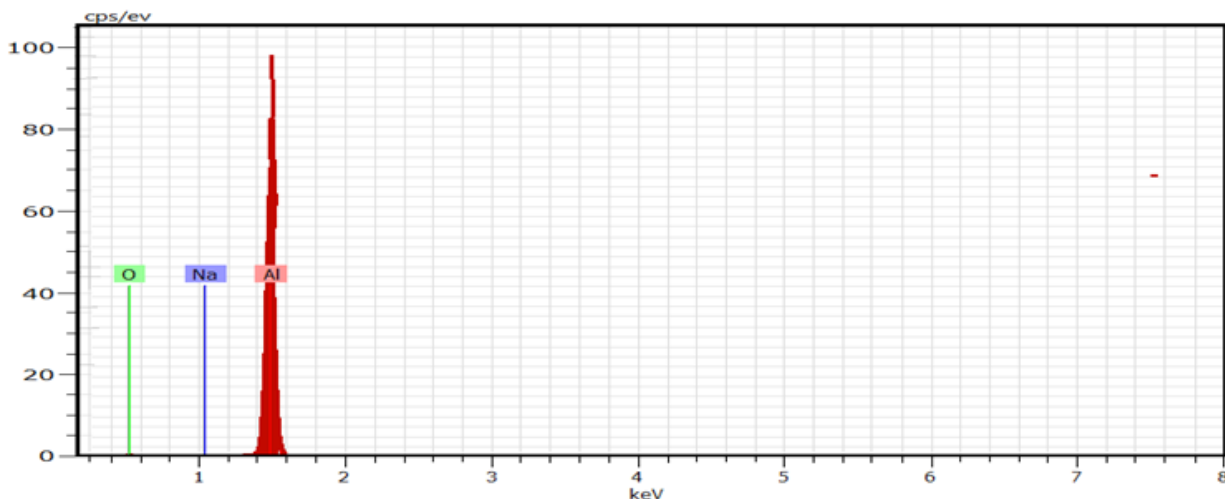
Figure 12. SEM micrographs of (a) polished metal; (b) Aluminium(6061) immersed in aqueous solution at pH 11; (c) Aluminium(6061) immersed in aqueous solution at pH 11 containing *o*-nitrophenol (250 ppm)+Zn²⁺ (50 ppm).

Energy Dispersive Analysis of X-rays (EDAX)

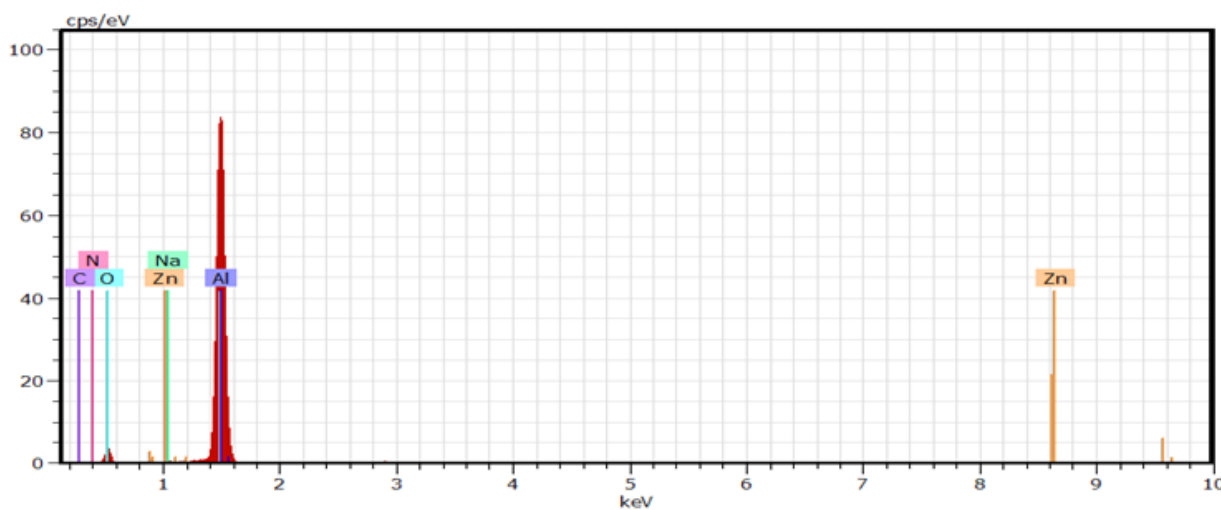
EDAX, usually performed in the presence and absence of inhibitor system is used to determine the elements present on the aluminium(6061) surface [28]. EDAX spectra is also used to confirm the results obtained from chemical and electrochemical measurements when a protective surface film of inhibitor is formed on the metal surface.

Figure 13(a) shows the EDAX analysis of aluminium(6061) surface immersed in aqueous solution at pH 11. The EDAX analysis shows the presence of characteristic peaks of corrosion product elements (Al, Na, O). Figure 13 represents the EDAX analysis of aluminium(6061) immersed in aqueous solution at pH 11 containing *o*-nitrophenol and 50 ppm of Zn²⁺. The analysis shows the presence of peak of zinc (Zn) which could be attributed to the presence of zinc and the inhibitor *o*-nitrophenol on the metal surface, forming a protective film. The surface of aluminium(6061) sample is preserved to a large

extent due to formation of the protective film of the inhibitor molecules as indicated by the decrease of aluminium(6061) peak in Figure 13(b).



(a)



(b)

Figure 13. EDAX spectra of (a) Aluminium(6061) immersed in aqueous solution at pH 11; (b) Aluminium(6061) immersed in aqueous solution at pH 11 containing *o*-nitrophenol (250 ppm)+Zn²⁺ (50 ppm).

The appearance of Zn peak and decrease in aluminium(6061) peak in the presence of an inhibitor indicated that the protective film formed is strongly adhered to the surface, leading to a high degree of *IE*. This result in the coordination of *o*-nitrophenol with Al³⁺, forming the *o*-nitrophenol–Al³⁺ complex on the anodic sites of the metal surface and the precipitation of zinc atoms as Zn(OH)₂ on the cathodic sites of the metal surface. There is also the possibility of deposition of Al(OH)₃.

Density Functional Theory

Computational methods

Accurate information about geometrical configuration, electron distribution and quantum chemical calculations were provided by Density Functional Theory (DFT) [29] which is an economic and efficient quantum chemistry computing method. It is widely applied in the analysis of corrosion inhibition performance and the interaction of corrosion inhibitors and interfaces [29]. The B3LYP functional was applied within the context of Gaussian 09 [30], using the 6-31+G(d,p) basis set. From quantum chemical study, the mechanism of corrosion, inhibitor adsorption on metal surfaces, and the merits of corrosion inhibitors can easily be studied. There is a correlation between experimental results and the quantum chemical parameters computed using DFT. The following quantum chemical indices were taken into consideration: the energy of the highest occupied molecular orbital (E_{HOMO}), the energy of the lowest unoccupied molecular orbital (E_{LUMO}), the energy band gap (ΔE), electron affinity (A), ionization potential (I), hardness (η), and softness ($1/\eta$).

The calculations were done by using the Gaussian 09 program. Schematic structures were drawn using the Chem Office package in the Ultra Chem 2010 version while optimized structures were drawn using the gauss View 5 program. The frontier molecule orbital density distributions of *o*-nitrophenol is presented in Figure 14. The calculated quantum chemical parameters are given in Table 6.

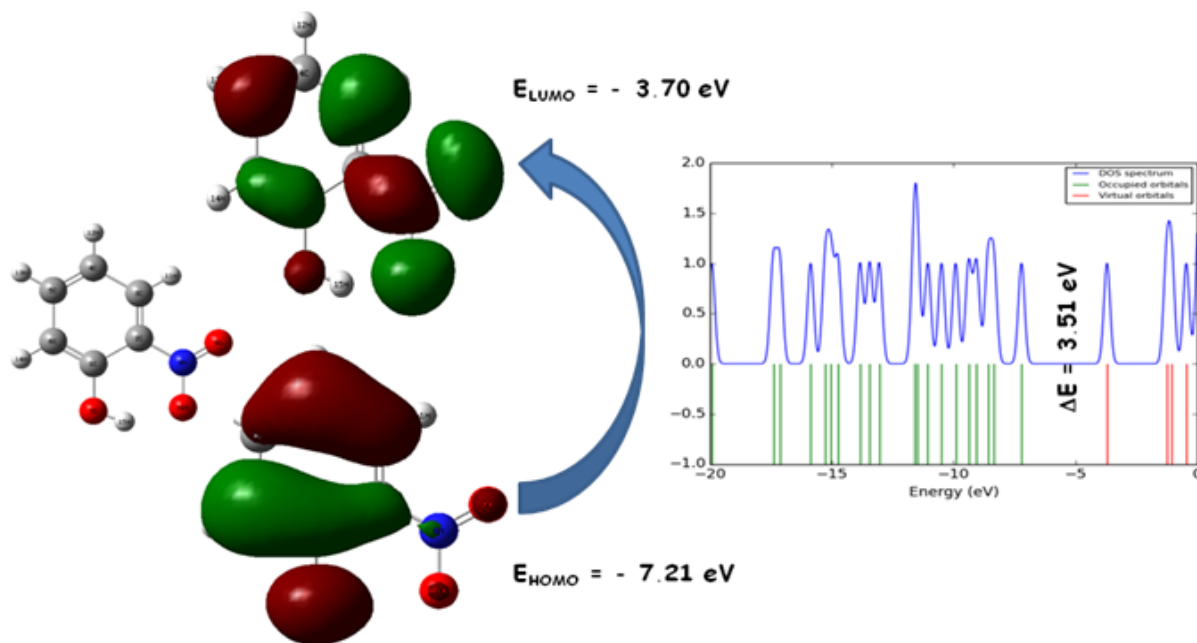


Figure 14. Schematic representation of HOMO and LUMO molecular orbital of *o*-nitrophenol.

Table 6. Calculated quantum chemical and corrosion parameters of the inhibitor *o*-nitrophenol molecule.

Parameters	<i>o</i> -nitrophenol
EHOMO	−7.21 eV
E_{LUMO}	−3.70 eV
$\Delta E E_{\text{LUMO}} - E_{\text{HOMO}}$	3.51 eV
Ionization Energy (I) ($-E_{\text{HOMO}}$)	7.21
Electron Affinity (A) ($-E_{\text{LUMO}}$)	3.70
Hardness (η) $I-A/2$	1.755
Softness (S) ($1/\eta$)	0.5698
IE % (weight loss method)	94
LPR, Ohm cm ²	1735.4
I_{corr} , A/cm ^{−2}	254.9×10^{-4}
R_t , Ohm cm ²	373.2
C_{dl} , F/cm ²	1.339×10^{-8}
Impedance value log(Z/Ohm)	2.790
RMS (R_q), nm	56.824
Average (R_a), nm	37.972
Maximum peak to valley height, nm	192.33

The inhibition effect is due to the adsorption of the inhibitor molecule on metal surface. Adsorption may be physical adsorption (physisorption) or chemical adsorption (chemisorption) depending on the adsorption strength. In chemisorption, one of the reacting species acts as an electron donor and the other one act as an electron acceptor. The energy of the highest occupied molecular orbital (E_{HOMO}) measures the tendency towards the donation of electron by a molecule [30]. High values of E_{HOMO} have a tendency of the molecule to donate electrons to appropriate acceptor molecules.

An inhibitor is not only an electron donor but also an electron acceptor. It can accept the electron from the d orbital of the metal leading to the formation of a feedback bond. The tendency for the formation of a feedback bond depend on the value of E_{LUMO} . The lower the E_{LUMO} , the easier is the acceptance of electrons from the d orbital of the metal.

Organic compounds, not only offer electrons to the unoccupied metal orbital but also accept free electrons from the metal. A molecule with a low energy gap is more polarizable and is generally associated with the high chemical activity and low kinetic stability and is termed soft molecule. Soft molecule is more reactive than a hard molecule because a hard molecule has a large energy gap.

Using the DFT/B3LYP method, the inhibition efficiency of *o*-nitrophenol molecule is investigated.

Acknowledgement

The authors are thankful to their respective management for their help and encouragement.

Conclusion

The present study leads to the following conclusions:

- i. The formulation consisting of 250 ppm of *o*-nitrophenol and 50 ppm of Zn^{2+} offers 94% *IE* to aluminium(6061) immersed in aqueous solution at pH 11 (NaOH) solution.
- ii. Polarization study reveals that *o*-nitrophenol (250 ppm) and Zn^{2+} (50 ppm) system controls the anodic reaction predominantly.
- iii. AC impedance spectra reveal the formation of protective film on the metal surface.
- iv. FTIR spectra reveal that the inhibitive film consists of Al^{3+} -*o*-nitrophenol complex on the metal surface. [Between pH 8 and 12 the ions polymerise by means of OH bridges and each aluminium is octahedrally coordinated. Thus $\text{Al}(\text{OH})_3$ dissolves in NaOH but is reprecipitated by the addition of carbon dioxide.]
- v. SEM and AFM images confirmed the protective film formed on the metal surface was smooth and stable.
- vi. EDAX indicates the elements of *o*-nitrophenol and Al^{3+} complex present on the anodic sites of the metal surface.
- vii. Density Functional Theory provides various quantum chemical parameters to study the inhibition efficiencies of various phenol inhibitors comparatively.

References

1. M.A. Abdel-Gaber, E. Khamis, S. Habo-Eidahab and Mh. Adeel, *Mater. Chem. Phys.*, 2008, **109**, 297.
2. E.I. Ating, S.A. Umoren, I.I. Udousoro, E.E. Ebenso and A.P. Udoh, *Green Chem. Lett. Rev.*, 2010, **3**, 61.
3. W.A. Badaway, F.M. AlKharafi and A.S. El-Azab, *Corros. Sci.*, 1999, **41**, 709.
4. R. Rosliza, W.B. Wan Nik and H.B. Senin, *Mater. Chem. Phys.*, 2008, **107**, 281.
5. A. Aytac, *J. Mater. Sci.*, 2010, **45**, 6812.
6. M. Gupta, J. Mishra and K.S. Pitre, *IJOART.*, 2014, **3**, 7.
7. V. Kalaivani, P.H. Arasu and S. Rajendran, *Int. J. ChemTech Res.*, 2013, **5**, no. 4, 1714.
8. V. Johnsirani, J. Sathiyabama and S. Rajendran, *Int. J. Nano Corr. Sci. Engg.*, 2016, **3**, no. 4, 115.
9. S. Shanmugapriya, S. Rajendran, P. Prabakar and N. Karthika, *Int. J. Nano Corr. Sci. Engg.*, 2016, **3**, no. 4, 144.
10. El-Sayed M. Sherif, *Int. J. Electrochem. Sci.*, 2011, **6**, 1479.

11. C.O. Akalezi, C.E. Ogukwe, E.A. Ejele and E.E. Oguzie, *Int. J. Corros. Scale Inhib.*, 2016, **5**, no. 2, 132. doi: [10.17675/2305-6894-2016-5-2-3](https://doi.org/10.17675/2305-6894-2016-5-2-3)
12. T.A. Onat, D. Yigit, H. Nazır, M. Güllü and G. Donmez, *Int. J. Corros. Scale Inhib.*, 2016, **5**, no. 3, 273. doi: [10.17675/2305-6894-2016-5-3-7](https://doi.org/10.17675/2305-6894-2016-5-3-7)
13. A.S. Fouda, M.A. El-Morsy, A.A. El-Barbary and L.E. Lamloum, *Int. J. Corros. Scale Inhib.*, 2016, **5**, no. 2, 112. doi: [10.17675/2305-6894-2016-5-2-2](https://doi.org/10.17675/2305-6894-2016-5-2-2)
14. V.I. Vigdorovich, L.E. Tsygankova, E.D. Tanygina, A.Yu. Tanygin and N.V. Shel, *Int. J. Corros. Scale Inhib.*, 2016, **5**, no. 1, 59. doi: [10.17675/2305-6894-2016-5-1-5](https://doi.org/10.17675/2305-6894-2016-5-1-5)
15. A. Anandan, S. Rajendran, J. Sathiyabama and D. Sathiyaraj, *Int. J. Nano Corr. Sci. Engg.*, 2016, **3**, no. 4, 9.
16. M. Lavanyaa and M. Suganya, *Int. J. Nano Corr. Sci. Engg.*, 2016, **3**, no. 4, 88.
17. P.N. Devi, J. Sathiyabama, S. Rajendran, R.J. Rathis and S.S. Prabha, *Int. J. Nano Corr. Sci. Engg.*, 2016, **3**, no. 4, 56.
18. S. Madhumitha, V. Priyadharshini, A. Sheela, C. Aadhithya, M. Sangeetha and S. Rajendran, *Int. J. Nano Corr. Sci. Engg.*, 2016, **3**, no. 4, 80.
19. P.N. Devi, J. Sathiyabama and S. Rajendran, *Int. J. Nano Corr. Sci. Engg.*, 2017, **6**, no. 1, 18.
20. D. Lakshmi, S. Rajendran and J. Sathiyabama, *Int. J. Nano Corr. Sci. Engg.*, 2016, **3**, no. 4, 181.
21. A. Selvan, *Int. J. Nano Corr. Sci. Engg.*, 2016, **3**, no. 4, 247. [21a] J.D.Lee, *Concise Inorganic Chemistry*, Third Edition, no. 160.
22. J. Telegdi, *Int. J. Corros. Scale Inhib.*, 2016, **5**, no. 4, 360. doi: [10.17675/2305-6894-2016-5-4-6](https://doi.org/10.17675/2305-6894-2016-5-4-6)
23. V.R.N. Banu and S. Rajendran, *Int. J. Nano Corr. Sci. Engg.*, 2016, **3**, no. 4, 312.
24. A.J. Vanitha, A.S. Raja and S. Rajendran, *Int. J. Nano Corr. Sci. Engg.*, 2016, **3**, no. 4, 223.
25. N.V. Tsirolnikova, Ya.V. Bolt, E.S. Dernovaya, B.N. Driker and T.S. Fetisova, *Int. J. Corros. Scale Inhib.*, 2016, **5**, no. 1, 66. doi: [10.17675/2305-6894-2016-5-1-6](https://doi.org/10.17675/2305-6894-2016-5-1-6)
26. W. Liu, A. Singh, Y. Lin, E.E. Ebenso, L. Zhou and B. Huang, *Int. J. Electrochem. Sci.*, 2014, **9**, 5574.
27. S.D. Meenakshi, S. Rajendran and J. Sathiyabama, *Int. J. Nano Corr. Sci. Engg.*, 2016, **3**, no. 4, 8.
28. D. Prabhu, Padmalatha, *Int. J. ChemTech Res.*, 2013, **5**, no. 6, 2690.
29. J.A. Thangakani, S. Rajendran and J. Sathiyabama, *Int. J. Nano Corr. Sci. Engg.*, 2016, **3**, no. 4, 280.
30. X. Pang, W. Guo, W. Li, J. Xie and B. Hou, *Sci. China Ser. B-Chem.*, 2008, **51**, no. 10, 928.

